Simple Expression for Estimating the Switch Peak Voltage on the Class-E Amplifier With Finite DC-Feed Inductance

Arturo Fajardo Jaimes*†
* Department of Electronics Engineering
Pontifical Xavierian University, Bogota, Colombia
Email: fajardoa@javeriana.edu.co

Fernando Rangel de Sousa †
† Radiofrequency Laboratory
Department of Electrical and Electronics Engineering
Federal University of Santa Catarina (UFSC), Florianpolis, Brazil
Email: rangel@ieee.org

***Abstract*—The class-E power amplifier is widely used due to its high efficiency, resulting from switching at zero voltage and zero slope of the switch voltage (i.e. ZVS and DZVS). This paper presents an analytical expression of the gain between the DC input voltage and the peak switch voltage on an ideal class-E power amplifier (PA) with finite dc-feed inductance, ZVS and DZVS operation. This expression is verified by simulations, and it is evaluated by experimental results at a switching frequency of 10.24MHz. Considering the results (simulated and experimental), the maximum error was 10,2%.**

Keywords*—*Class-E, power amplifier, power efficiency, wireless power transfer.

I. INTRODUCTION

The Class-E power amplifier (PA) has been extensively studied and many different aspects of it has been analyzed. In particular, the ideal Class-E PA (i.e. Fig. 1(a)) with a finite dc-feed inductance instead of an RF-choke in a Class-E PA has been explored [1]–[5]. For the same supply voltage, output power and load, using finite dc-feed inductance has significant benefits [6]: more efficient output matching network, implementation in low-voltage technologies and higher frequency of operation. The published papers about this PA can be categorized, considering the design approach, in two main groups: based on analytical equations [3], [5], [6] and based on iterative procedures [1], [4]. Further, when the switch on-resistance and the inductor resistance are taken into account, the class-E PA solution results in complicated nonlinear analytic equations that must be solved numerically [7], [8] or in iterative design procedures even more lengthy and complex [9], [10]. Furthermore, the optimum operation of the class-E PA occurs at the non-nominal operation (i.e. without ZVS and DZVS) [10]. An intermediary solution was proposed in [11], they used the analytical solution of the ideal class-E PA equations as the first point of an iterative procedure for solving the optimization of the PA.

Considering the Class-E PA presented in the Fig. 1(a), the peak value of the switch voltage should be lower than the breakdown voltage of the transistor. The solutions for alleviating this problem include [7]: parallel structures and power combining, cascode switching, combining with class-F/F^{-1}, and designing for sub-optimum or off-nominal operation of the class-E PA. The published design methodologies for nominal or optimum operation that consider the switch breakdown voltage (V_{S_M}) involves hard simulation work [10] or numerical method solution of non-linear equations [7]. On the other hand, in [11] was included the V_{S_M} in an analytical design set, this set was divided in specification gains and circuit element gains as is illustrated in the Fig.2(a). The specification gains were used to calculate the design space of the class-E PA based in the inputs and outputs constrains, and the circuit element gains were used for calculating the circuit components. All of these gains are analytic functions of the input variables, therefore the design set can be implemented and calculated in any math software for analyzing all the involved trade-offs. As an example of this approach, the design space of the PA designed in [11] was plotted in the Fig. 2(b).

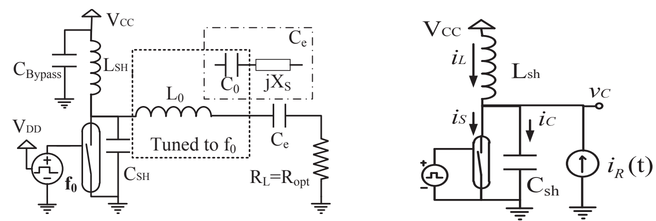

(a) Ideal model (b) Model High Q

Fig. 1. Class-E PA

This paper presents the synthesis of the analytic relationship between the DC input voltage and V_{S_M} on a class-E PA with finite dc-feed inductance used in [11].

II. IDEAL NOMINAL CLASS-E MODEL

The ideal class-E PA circuit shown in Fig.1(a) can be modeled as the circuit shown in Fig. 1(b) when the control

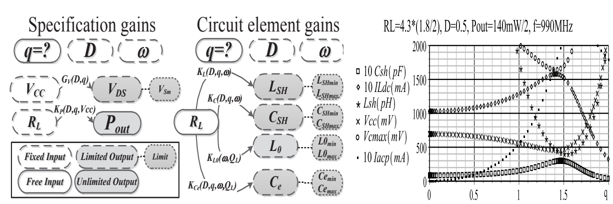

(a) Gains (b) Design Space

Fig. 2. Ideal class-E design set.

$$0 = \cos(q\theta_m)\sin(2\pi q)\cos(\varphi)\,pq^2 - \cos(2\pi q)\sin(q\theta_m)\cos(\varphi)\,pq^2 - \sin(2\pi q)\sin(q\theta_m)\sin(\varphi)\,pq + \cos(q\theta_m)\sin(2\pi q)\,q^2 + pq\sin(\theta_m+\varphi) - \cos(q\theta_m)\sin(2\pi q) + \cos(2\pi q)\sin(q\theta_m) - \cos(q\theta_m)\cos(2\pi q)\sin(\varphi)\,pq - \cos(2\pi q)\sin(q\theta_m)\,q^2 \quad (14)$$

signals has 0 time transitions at a frequency f (near to f_0) and the series resonant circuit L_0, C_e and R_L has a high loaded quality factor. Therefore, the output current is given by (1). As a result of development presented presented in [5], for ideal class-E nominal operation (i.e. with ZVS and DZVS), the PA currents and PA voltages, are given by the equations (2) to (7).

$$i_R(t) = I_P sin(\omega t + \varphi) = \sqrt{\frac{2P_{OUT}}{R_L}} sin(2\pi f t + \varphi); \quad (1)$$

$$v_{C_{SH_{on}}}(t) = i_{C_{SH_{on}}}(t) = i_{S_{off}}(t) = 0; \quad (2)$$

$$i_{L_{SH_{on}}}(t) = \frac{V_{CC}}{L_{SH}} t - I_P sin(\varphi); \quad (3)$$

$$i_{S_{on}}(t) = \frac{V_{CC}}{L_{SH}} t + I_P (sin(\omega t + \varphi) - sin(\varphi)); \quad (4)$$

$$v_{C_{SH_{off}}}(t) = \begin{array}{c} V_{CC} + C_1\cos(q\omega t) + C_2\sin(q\omega t) \\ -\frac{q^2}{1-q^2} p V_{CC}\cos(\omega t + \varphi); \end{array} \quad (5)$$

$$i_{C_{SH_{off}}}(t) = \begin{array}{c} \frac{V_{CC}}{L_{SH}} t - \frac{1}{L_{SH}} \int_{\frac{2\pi D}{\omega}}^{t} v_{C_{SH}}(\tau) d\tau \\ + I_P (sin(\omega t + \varphi) - sin(\varphi)) \end{array}; \quad (6)$$

$$i_{L_{SH_{off}}}(t) = \frac{V_{CC}}{L_{SH}} t - \int_{\frac{2\pi D}{\omega}}^{t} \frac{v_{C_{SH}}(\tau)}{L_{SH}} d\tau - I_P sin(\varphi); \quad (7)$$

where, X_{on} means that the expression X is valid when the switch is in the ON state ($0 < t < \frac{2\pi D}{\omega}$). On the other hand, X_{off} means that the expression X is valid when the switch is in the OFF state ($\frac{2\pi D}{\omega} < t < \frac{2\pi}{\omega}$). The constants C1 and C2 are analytic functions of p,q,φ and V_{DD}, and they were found in [5]. The variables p and q were introduced by [5], in order to simplify the math analysis and are defined as:

$$q = \frac{1}{\omega\sqrt{L_{SH}C_{SH}}} = \frac{\omega_{SH}}{\omega}; p = \frac{\omega L_{SH} I_P}{V_{CC}} = \frac{Z_{L_{SH}}}{R_\omega}; \quad (8)$$

where, ω_{SH} is the parallel tuned frequency of the LC_{SH} network , Z_{LSH} is the impedance of L_{SH}, and R_ω is:

$$R_\omega = \frac{V_{CC}}{I_P} = \sqrt{\frac{P_{in}R_{DC}}{2P_{out}/R_L}} = \frac{\sqrt{R_L R_{DC}}}{\sqrt{2}}; \quad (9)$$

where, R_L is the PA load , P_{in} is the power delivered by V_{CC}, P_{out} is the power dissipated by R_L, and R_{DC} is the equivalent resistance (introduced by [11]) that the amplifier imposes to V_{CC} and can be calculated as:

$$R_{DC} = \frac{V_{DC}}{I_{DC}} = V_{CC} \Big/ \frac{\omega}{2\pi} \int_0^{\frac{2\pi}{\omega}} i_s(t) dt = \frac{R_\omega}{g}; \quad (10)$$

therefore, from (10) and (9), the R_{DC} can be rewritten as:

$$R_{DC} = R_L / 2g^2 \quad (11)$$

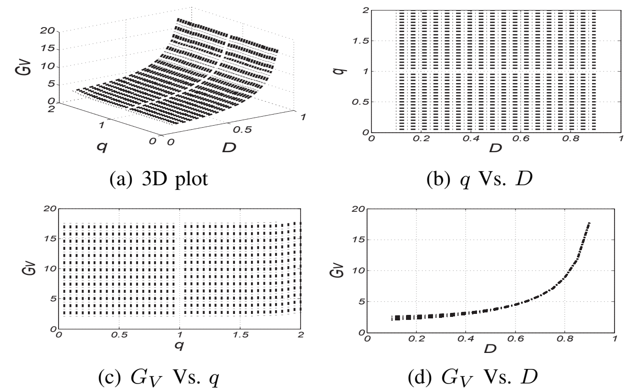

(a) 3D plot (b) q Vs. D (c) G_V Vs. q (d) G_V Vs. D

Fig. 3. Peak voltage gain (G_V) for the ideal class-E PA

where,

$$g(q,D) = \left\{ \begin{array}{c} \left(\frac{1-\cos(2\pi D)}{2\pi}\right)\cos(\varphi) \\ + \left(\frac{\sin(2\pi D)}{2\pi} - D\right)\sin(\varphi) + \frac{D^2\pi}{p} \end{array} \right\}. \quad (12)$$

It is important to emphasize that the expressions from (1) to (12) can be calculated in terms of V_{CC}, ω, R_L, and P_{OUT} only if p,q,φ and D are known, but in [5] was demonstrated that both φ and p could be solved as a analytic function of both q and D.

III. Ideal class-E PA switch breakdown voltage

A. Numerical solution

The peak value of the switch voltage occurs when:

$$\frac{d}{dt} V_C(\omega t_{max}) = 0; \quad (13)$$

where, t_{max} is the time at which the peak value occurs. From (5) and (13) it was found (14) (i.e. the equation at the top of the page). Solving numerically this equation, the ωt_{max} value is calculated in function of the parameter values q and D, using ωt_{max} the peak value of the switch voltage value gain ($G_V(q,D) = \frac{V_{c_{max}}}{V_{CC}}$) was found from (6), and the results were plotted in the Fig.3.

B. Curve fitting

As a simplified approach, the variation on G_V gain with respect to changes in the q variable can be neglected, therefore this gain was assumed as:

$$G_V a(D,q) = \frac{a}{1-D}; \quad (15)$$

where, a is a constraint value that minimizes the involved error. The fitting error was defined following the percentage least squares criteria as:

$$E_k = \frac{(G_V a(q_i, D_j) - G_V(q_i, D_j))}{G_V(q_i, D_j)} \quad (16)$$

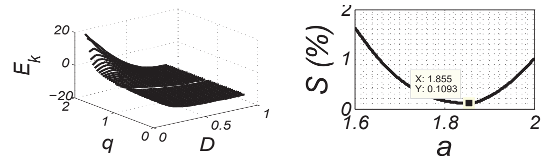

(a) Error 3D plot (b) S Vs. a

Fig. 4. Least squares fitting

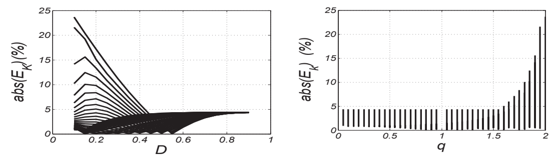

(a) E_k Vs. D (b) E_k Vs. Q

Fig. 5. Least squares error for a=1.8551

where q_i is the sample i of the q variable and q_j is the sample j of the D variable, and E_k is the error value for the sample (i, j). The goal function (S) was defined as:

$$S(a) = \sum_k \frac{{E_k}^2}{n} \tag{17}$$

where, n is the number of samples of the numerical solution. Therefore, the optimum value of a minimizes the sum of the calculated error squares for all the samples. The optimization process is illustrated in the Fig. 4(b). The error function for this optimum value was plotted in Fig.4(a). Using the optimum value, (15) can be rewritten as:

$$G_V a(D, q) = \frac{1.8551}{1-D}. \tag{18}$$

In order to analyze this results, the absolute value of the percentage error was plotted in Fig.5. Considering this figure, the approximation error is less than 5% for any D value and a q less than 1.7. For large q (i.e. $q > 1.65$) the values of either input parameters or circuit elements correspond to extreme values [6]. Hence, we focus on q values lower than 1.7. The mean perceptual error for the limited range ($0 < q < 1.7, 0 < D < 1$) was 3%, and the maximum perceptual error was 7%. Further, a similar optimization procedure was made. Therefore, (15) can be rewritten as:

$$G_V a(D, q) = \frac{1.8208}{1-D}; \tag{19}$$

the absolute value of the new percentage error was plotted in Fig.6. Considering this figure, the approximation error is less than 5.3% for any D value and a q less than 1.5. The mean perceptual error in all the range ($0 < q < 1.7, 0 < D < 1$) was 2%, and the maximum perceptual error was 8.8%.

In order to reduce the approximation error in the peak value prediction, for a fixed duty cycle ($D = D_x$), the approximative expression may be refined using a polynomial c(x) of degree n of the variable q that fits the data, in the least squares sense. Therefore (15) can be rewritten as:

$$G_V a(D_x, q) = \frac{c(q)}{1-D_x} = \frac{c_0 + c_1 q + \cdots + c_n q^n}{1-D_x}; \tag{20}$$

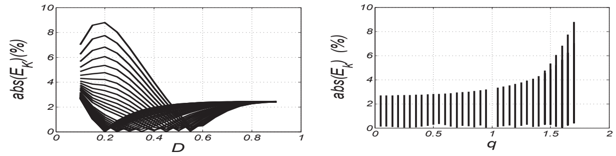

(a) E_k Vs. D (b) E_k Vs. Q

Fig. 6. Least squares error for a=1.8208

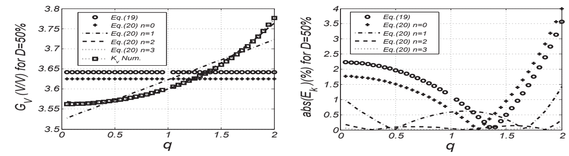

(a) G_V Vs. q (b) E_k Vs. Q

Fig. 7. Polynomial fitting of G_V for D=50%

using a duty cycle of 50%, the error can be decreased as is presented in the Fig.7. Hence, using n=2, (20) can be rewritten as:

$$G_V a(D_x, q) = \frac{1.7613 + 0.0500q}{1-D_x}; \tag{21}$$

this expression has perceptual error of less than 2% in all the range ($0 < q < 2, D = 50\%$).

IV. Using the CLASS-E design set

The relations between the input parameters (Q_L,V_{CC}, P_{OUT} and ω) and the circuit element values (L_{SH}, C_{SH}, C_e, L_0 and R_L) should be known. These relations are commonly referenced as the design set, in this paper we use the set proposed in [5] and extended in [11]. This set is summarized in the table I.

TABLE I. Circuit element gains

$K_P(q, D, V_{CC}, R_L) = Pout/R_L = 2g(q, D)^2 \left(\frac{V_{CC}}{R_L}\right)^2$
$K_{C^{-1}}(q, D, \omega) = (C_{SH})^{-1}/R_L = \frac{q^2 p(q,D)}{2g(q,D)}(\omega)$
$K_L(q, D, \omega) = L_{SH}/R_L = \frac{p(q,D)}{2 \cdot g(q,D)}\left(\frac{1}{\omega}\right)$
$K_{X_S} = (q, D) = \frac{X_s}{R_L} = \frac{v_{C_I}/i_{R_Q}}{v_{C_Q}/i_{R_Q}} = \frac{\left(\frac{-2}{I_P T}\int_0^T v_C(t)\cos(\omega t+\varphi)dt\right)}{\left(\frac{-2}{I_P T}\int_0^T v_C(t)\sin(\omega t+\varphi)dt\right)}$
$K_{L_0}^{-1}(\omega, Q_L) = L_0/R_L = \frac{Q_L}{\omega}$
$K_{C_0^{-1}}(\omega, Q_L) = (C_0)^{-1}/R_L = Q_L\omega$
$K_{C_e^{-1}}(\omega, Q_L, q, D) = (C_e)^{-1}/R_L = \omega\left(Q_L - K_{X_s}(q, D)\right)$

V. Measurement and simulated results

In order to verify (19), (21) and (11), a PA was simulated following the specifications summarized in Table II. The simulation setup uses the harmonic balance simulation technique in the Advanced Design System (ADS®) software. Furthermore, the transistor is represented as a voltage controlled switch model, with ideal control signal (with 0 time transitions at a frequency f), an on resistance of 1 mΩ, and an open resistance of 100 GΩ. All the other circuit elements are simulated as ideal components. In order to calculate its values, first the relations that are only dependent on the q and D specification were

TABLE II. SPECIFICATIONS FOR THE CLASS-E PA

q	D (%)	f (MHz)	V_{CC} (V)	Q_L	R_L (Ω)
0.8,1.412,1.65	50	10,24	2	100,10,6	22

TABLE III. RELATIONS THAT ARE ONLY FUNCTIONS OF q AND D

D=50% q	p (D,q)	ψ (D,q)	g (D,q)	K'_P $2g^2_{(q,D)}$	K'_L $\frac{p(q,D)}{2\cdot g(q,D)}$	K'_C $\frac{q^2 p(q,D)}{2g(q,D)}$	K_{X_S} (D,q)
0.8	7.0850	-0.4446	0.6133	0.7522	5.7760	0.2705	0.8907
1.412	1.3630	0.2640	0.8256	1.3630	0.7332	0.6841	-0.0002
1.65	0.9196	0.9706	0.6213	0.7719	0.7401	0.4963	-0,8817

calculated (summarized in the Table III), then following the circuit element gains of the design set and the Q_L specification, the circuit values were calculated and summarized in Table IV.

The experimental results are taken from [6], where discrete Class-E PAs were constructed with a transistor (MAX 2601), and discrete passive components. Further, the transistor gate was driven by a square wave signal from the signal source. The rise and fall time was chosen as 10 % of the period of the square signal (10.24 MHz). These simulated and experimental results are summarized in Table V. In the Table VI both the mean and the maximum percentage error was calculated for the analyzed variables. Considering this table, the predicted error involved in the expression analyzed (i.e. (19), (21) and (11)) is less than 20% including simulated and experimental results. Futher, the minimum error prediction of the G_V is achieved using (19), because the unmodeled dynamics (i.e. finite Q_L) increase the error of the numerical solution, as is clear from the increase of the error with a lower value of Q_L. From these analysis, the equation (19) is a simple appropriate expression for modeling G_V. When (11) was used for the R_{DC} prediction, the maximum error found was 18.02%, this is because is more sensitive to the unmodeled losses, that impacts in the experimental results.

VI. CONCLUSIONS

An analytical expression of the gain between the DC input voltage and the peak switch voltage on a ideal class-E power amplifier (PA) for a finite dc-feed inductance and ZVS and DZVS operation was presented. This expression was verified by the simulations, and was evaluated by experimental results ($f = 10.24$ MHz), with good agreement between the results and the predicted values. Considering the simulated and experimental results the maximum predicted error was 10,2%.

ACKNOWLEDGMENT

The first author would like to thank COLCIENCIAS and the Pontificia Universidad Javeriana for the financial support.

TABLE IV. CALCULATED CIRCUIT VALUES

	L_0 (uH)	C_0 (pF)	C_e (pF) (D=0.5, q=0.8)	q=1.412)	q=1.65)	L_{SH} (nH)	C_{SH} (pF)
Q=6	2.052	117.746	138.271	117.743	102.659	1975	191.097
Q=10	3.419	70.648	77.555	70.646	64.923	250.691	483.317
Q=100	34.193	7.065	7.128	7.065	7.003	253.066	350.622

TABLE V. CLASS-E PA RESULTS

q	Paremeter	Theoric	Sim. (QL=100)	Sim. (QL=10)	Sim. (QL=6)	Meas. (QL=6)
0.8	P_{out} (mW)	136.8	138.0	141.0	144.0	96.6
	P_{DC} (mW)	136.8	138.0	141.0	145.0	114.8
	Drain η (%)	100.0	99.9	99.8	99.3	84.1
	G_V (Num,Eq19,Eq21) (V/V)	3.59 3.64 3.60	3.60	3.72	3.81	3.35
	V_{S_M} (Num,Eq19,Eq21) (V)	7.17 7.28 7.21	7.20	7.44	7.62	6.70
	R_{DC} (Ω)	29.2	29.0	28.3	27.7	34.8
1.412	P_{out} (mW)	247.9	249.0	252.0	255.0	171.1
	P_{DC} (mW)	247.9	249.0	253.0	256.0	203.2
	Drain η (%)	100.0	99.9	99.8	99.6	84.2
	G_V (Num,Eq19,Eq21) (V/V)	3.65 3.64 3.66	3.66	3.72	3.77	3.33
	V_{S_M} (Num,Eq19,Eq21) (V)	7.29 7.28 7.33	7.32	7.44	7.55	6.65
	R_{DC} (Ω)	16.1	16.1	15.8	15.6	19.7
1.65	P_{out} (mW)	140.4	141.0	145.0	149	103.5
	P_{DC} (mW)	140.4	141.0	145.0	150	134.2
	Drain η (%)	100.0	99.9	99.7	99.1	77.1
	G_V (Num,Eq19,Eq21) (V/V)	3.69 3.64 3.69	3.70	3.83	3.93	3.45
	V_{S_M} (Num,Eq19,Eq21) (V)	7.37 7.28 7.38	7.40	7.65	7.86	6.90
	R_{DC} (Ω)	28.5	28.4	27.5	26.7	29.8

TABLE VI. ERROR RESULTS

Error (%)	G_V or V_{S_M} Num	Eq19	Eq21	RDC	q 0.80	1.412	1.65	QL 100	10	6
Mean	5.98	6.40	6.10	9.52	4.46	4.10	4.36	0.51	2.95	9.42
Max	9.68	9.52	10.20	18.02	16.06	18.02	7.36	1.55	4.83	18.02

REFERENCES

[1] R. Zulinski and J. W. Steadman, “Class e power amplifiers and frequency multipliers with finite dc-feed inductance,” *IEEE Trans. Circuits Syst.*, vol. 34, no. 9, pp. 1074–1087, Sep 1987.

[2] C.-H. Li and Y. Yam, “Maximum frequency and optimum performance of class e power amplifiers,” *IEE Proc. on Circuits, Devices and Systems*, vol. 141, no. 3, pp. 174–184, Jun 1994.

[3] D. Choi and S. Long, “Finite dc feed inductor in class e power amplifiers-a simplified approach,” in *IEEE MTT-S Int. Microwave Symp. Dig.*, vol. 3, June 2002, pp. 1643–1646 vol.3.

[4] D. Milosevic, J. van der Tang, and A. van Roermund, “Explicit design equations for class-e power amplifiers with small dc-feed inductance,” in *Proc. of the European Conf. on Circuit Theory and Design*, vol. 3, Aug 2005, pp. III/101–III/104 vol. 3.

[5] M. Acar, A. Annema, and B. Nauta, “Analytical design equations for class-e power amplifiers,” *IEEE Trans. Circuits Syst. I, Reg. Papers*, vol. 54, no. 12, pp. 2706–2717, Dec 2007.

[6] ——, “Generalized design equations for class-e power amplifiers with finite dc feed inductance,” in *36th European Microwave Conference*, Sept 2006, pp. 1308–1311.

[7] R. Sadeghpour and A. Nabavi, “Design procedure of quasi-class-e power amplifier for low-breakdown-voltage devices,” *IEEE Trans. Circuits Syst. I, Reg. Papers*, vol. 61, no. 5, pp. 1416–1428, May 2014.

[8] M. Acar, A. Annema, and B. Nauta, “Analytical design equations for class-e power amplifiers with finite dc-feed inductance and switch on-resistance,” in *IEEE Int. Symp. on Circuits and Systems*, May 2007, pp. 2818–2821.

[9] R. Zhang, M. Acar, M. Apostolidou, M. van der Heijden, and D. Leenaerts, “Concurrent l- and s-band class-e power amplifier in 65nm cmos,” in *IEEE Radio Frequency Integrated Circuits Symp.*, June 2012, pp. 217–220.

[10] N. Sokal and A. Mediano, “Redefining the optimum rf class-e switch-voltage waveform, to correct a long-used incorrect waveform,” in *IEEE MTT-S Int. Microwave Symp. Dig.*, June 2013, pp. 1–3.

[11] A. Fajardo and F. Rangel de Sousa, “Integrated cmos class-e power amplifier for wireless power transfer,” presented at the IEEE Int. Symp. on Circuits and Systems, Montreal, Canada, 2016.